Receptor Scintigraphy with a Radioiodinated Somatostatin Analogue: Radiolabeling, Purification, Biologic Activity, and In Vivo Application in Animals

Willem H. Bakker, Eric P. Krenning, Wout A. Breeman, Jan W. Koper, Peter P. Kooij, Jean-Claude Reubi, Jan G. Klijn, Theo J. Visser, Roel Docter, and Steven W. Lamberts

Departments of Nuclear Medicine and Internal Medicine III, University Hospital Dijkzigt and Erasmus University Medical School, Rotterdam, The Netherlands; Division of Endocrine Oncology, Dr. Daniel den Hoed Cancer Centre, Rotterdam, The Netherlands; and Sandoz Research Institute, Berne, Switzerland

Radioiodinated Tyr-3-octreotide, a somatostatin analogue, is a useful ligand for the in vitro detection of somatostatin receptors. In this study, we have investigated the possible in vivo application of this radioligand in the detection of somatostatin receptor-bearing tumors by scintigraphy. The specific somatostatin-like biologic activity of radioiodinated Tyr-3-octreotide was confirmed in vitro: (a) radioiodinated Tyr-3-octreotide competes in the nanomolar range with specific receptor binding of somatostatin to suspended human meningioma membranes and (b) the secretion of growth hormone by cultured rat pituitary cells was similarly inhibited by iodinated Tyr-3-octreotide and somatostatin. In rats, intravenously injected ^{123}I-Tyr-3-octreotide is rapidly cleared from the circulation mainly by the liver. Although this rapid clearance limits the amount of tracer available for somatostatin receptor-bearing tumors, the advantage of this rapid clearance is that the background level is rapidly reduced in favor of scintigraphic imaging of these tumors. Pancreatic tumors in rats were localized by scintigraphy after intravenous injection of ^{123}I-Tyr-3-octreotide.

J Nucl Med 1990; 31:1501–1509

Most endocrine active gastrointestinal tumors are usually slow-growing. They are often very small and therefore difficult to localize with conventional techniques (*1*). Hormone secretion by several of these tumors is inhibited by the tetradecapeptide somatostatin (Fig. 1A), which is endogenously produced, e.g., by the hypothalamus and pancreas (*2*). Somatostatin also inhibits the growth of some tumors (*3*). The native hormone, however, is susceptible to rapid enzymatic degradation (*4*); therefore, it is not suitable for long-term therapeutic use. For that reason, synthetic derivatives with a similar bioactive structure as somatostatin have been developed, which are not only less susceptible to biologic degradation but also have a stronger inhibitory effect on hormone release by the relevant tumors. The octapeptide octreotide (SMS 201-995 or Sandostatin®; Fig. 1B) fulfils these criteria (*4*). After subcutaneous injection, this peptide has a longer biologic half-life than somatostatin itself and, hence, prolonged inhibitory effects on normal growth hormone production (*5*), hormone release by endocrine pancreatic tumors (*6*), and on tumor growth (*6–9*). Octreotide is currently used in the treatment of gastroenteropancreatic tumors and acromegaly (*6,10*).

Large numbers of high-affinity binding sites for native somatostatin and synthetic octreotide have been detected on most endocrine active tumors (*11*). This opens the possibility for the scintigraphic localization of such tumors using a radiolabeled somatostatin derivative. Since octreotide cannot be radiolabeled easily with a gamma-emitting radionuclide, a synthetic analogue (Tyr-3-octreotide) has been developed in which phenylalanine has been replaced by tyrosine, allowing radioiodination of the molecule (Fig. 1C). This compound has been used successfully as an iodine-125-(^{125}I) radioligand for in vitro somatostatin receptor studies (*12*). Since its application for human scintigraphy needs methodologic changes (use of ^{123}I with different properties instead of ^{125}I and omitting toxic substances during purification), we report here the radiolabeling, the subsequent purification procedure, and the confirmation of the specific biologic activity of radiolabeled Tyr-3-octreotide. The distribution and metabolism of the radiolabeled somatostatin derivative have been studied following its intravenous administration to rats by gamma camera scintigraphy and measurements of

Received Sept. 21, 1989; revision accepted Mar. 5, 1990.

For reprints contact: Willem H. Bakker, University Hospital Dijkzigt, Department of Nuclear Medicine, Dr. Molewaterplein 40, 3015 GD Rotterdam, The Netherlands.

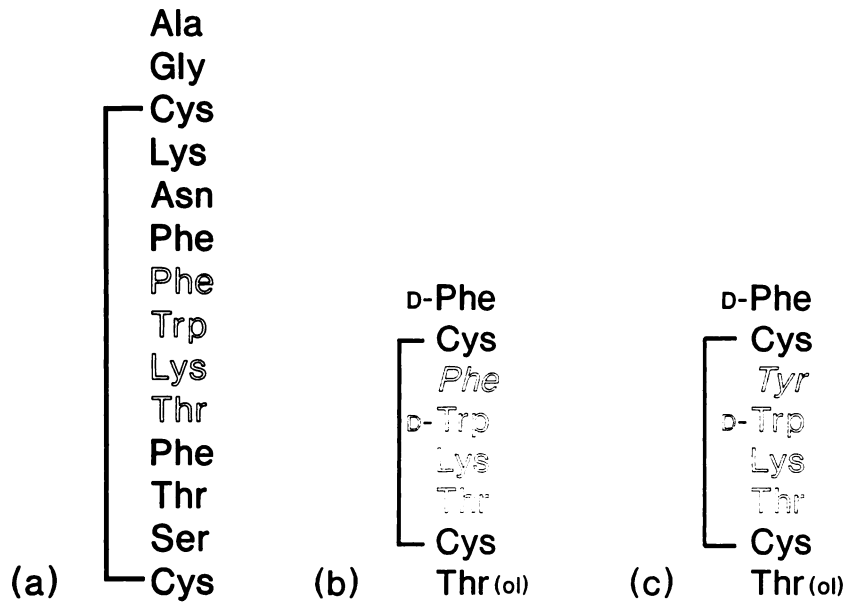

FIGURE 1
Structural formulae of native somatostatin (a) with the Phe-Trp-Lys-Thr sequence, which has been proposed to be the active site of the molecule (*23*, *24*) and octreotide (b). In Tyr-3-octreotide (c) Phe is replaced by Tyr to make radioiodination possible with preservation of biologic activity.

radioactivity in isolated organs. Radioiodinated Tyr-3-octreotide was shown to be an attractive new radiopharmaceutical for the in vivo detection of somatostatin receptors using a rat tumor model.

MATERIALS AND METHODS

Radiopharmaceuticals

Octreotide and Tyr-3-octreotide were obtained from Sandoz (Basel, Switzerland). Radioiodination of Tyr-3-octreotide was performed on the basis of the ^{125}I-iodination technique described by Reubi (*12*). Toxic substances were omitted during the purification steps in connection with the proposed i.v. administration. Two iodine isotopes (^{125}I and ^{123}I) from different manufacturers were used. Radioactivity concentrations (and specific activities) amounted to 1.85 GBq ^{125}I/ml (0.62 TBq ^{125}I/mg) and 3.7 GBq ^{123}I/ml (3.7 TBq ^{123}I/mg). To the solution of radioiodide (in 40 μl 0.01 *M* NaOH) in the manufacturer's vial were added successively 20 μl 0.05 *M* phosphate (pH 7.5) and 1.4 μg Tyr-3-octreotide in 20 μl 0.05 *M* acetic acid. The solution was vortexed. The iodination was started by adding 1.6 μg chloramine-T (in 20 μl 0.05 *M* phosphate), representing only a 5-fold excess over peptide in order to prevent oxidation of the disulfide bridge of the Tyr-3-octreotide. The mixture was then vortexed for 1 min. The iodination wa stopped by the addition of 0.1 ml 10% human serum albumin (Merieux, Lyon, France). After vortexing for 30 sec, 1.85 ml 5 m*M* ammonium acetate was added. Purification was performed by using a SEP-PAK C18 reversed-phase extraction cartridge (Waters Associates, Milford, MA), which was prewashed with 5 ml 70% ethanol and subsequently activated with 5 ml 2-propanol. After application of the sample, the cartridge was washed successively with 5 ml distilled water and 5 ml 0.5 *M* acetic acid. Radioiodinated Tyr-3-octreotide was eluted with 5 ml 96% ethanol. The solvent was evaporated at 40 °C under a gentle stream of nitrogen. The dry residue was dissolved in 2–10 ml 154 m*M* NaCl and 0.05 *M* acetic acid (pH 3). After passing through a low protein-binding 0.22-micron Millex-GV filter (Millipore, Milford, MA), the solution was ready for i.v. administration. The labeling procedure was scaled up at least 30-fold when larger amounts of radiolabeled peptide were necessary for (human) scintigraphic purposes. In those cases, 10-fold higher peptide- and chloramine-T concentrations were used in order to keep the reaction volume below 1 ml. For labeling with ^{125}I and ^{123}I, 1.5- and 30-fold excess of peptide over iodide were used, respectively.

Quality Control

The radioactivities in the fractions eluted from SEP-PAK C18 were measured in a dose calibrator (VDC, 202, Veenstra, Joure, The Netherlands) under similar geometric conditions (5 ml liquid). Also, the SEP-PAK C18 cartridge itself was measured after the elutions, taking into account the different geometric conditions.

The ammonium acetate, water, and acetic acid fractions eluted from SEP-PAK C18 were examined for low molecular weight (<1.5 kD) iodine (i.e., free iodide and peptide-bound radioiodine) and high molecular weight (>1.5 kD) protein-bound iodine (i.e., radioiodinated human serum albumin) using Sephadex G-25 gel filtration chromatography (PD-10 column, Pharmacia, Sweden) with 154 m*M* NaCl as the eluent. The low molecular weight PD-10 fractions were analyzed by reversed-phase, high-performance liquid chromatography (HPLC), described hereafter.

The acetic acid and ethanol fractions eluted from SEP-PAK C18 were analyzed by HPLC with a Waters 600 E multisolvent delivery system connected to a μ-Bondapak-C18 reversed-phase column (300 × 3.9 mm, particle size 10 μm). Elution was carried out at a flow of 1 ml/min with a linear gradient of 40% to 80% methanol in 154 m*M* NaCl in 20 min and the latter composition was maintained for another 5 min. Eluted radioactivity was monitored on-line using a NaI probe connected to a Canberra single-channel analyzer with a recorder. Collected fractions were measured by routine scintillation counting.

The receptor-binding affinity of the radioiodinated Tyr-3-octreotide was measured using suspensions of human menin-

gioma membranes, which are reported to contain somatostatin receptors (*13*). A similar procedure as described previously (*12*) was used. Meningioma membranes (280 μg protein) were incubated in a total volume of 100 μl (triplicate tubes) at 20°C for 1 hr with five different concentrations of ^{123}I-Tyr-3-octreotide between 0.2 and 8 n*M* in the absence or presence of 10 μ*M* somatostatin. The incubation contained 10 m*M* HEPES buffer (pH 7.6), 0.5% BSA, 5 m*M* $MgCl_2$, and bacitracin (20 μg/ml). The incubation was stopped by the addition of 1 ml ice-cold HEPES buffer followed by centrifugation (2 min at 14,000 rpm in an Eppendorf microcentrifuge). The membrane pellet was washed twice with 1 ml ice-cold HEPES buffer and the final pellet was counted in a LKB-1282-Compugamma system. Specific receptor binding was calculated to be the difference between binding in the absence and in the presence of 10 μ*M* somatostatin. The data were analyzed using the method of Scatchard (*14*), giving the dissociation constant (K_d) and the number of binding sites (B_{max}) for the meningioma preparation.

The biologic activity of HPLC-purified mono-iodinated ^{125}I-Tyr-3-octreotide (i.e., free from unlabeled Tyr-3-octreotide) was assessed by measuring its potency to inhibit the secretion of rat growth hormone (rGH) by cultured rat pituitary cells as described previously (*15*). Iodine-125 was used instead of ^{123}I because we were only able to establish the exact specific radioactivity of the ^{125}I-Tyr-3-octreotide (see Discussion).

Animals and Tumors

A transplantable rat pancreatic tumor model (CA 20948) with somatostatin receptors, as demonstrated with in vitro assays (*16*), was used. Inhibition of the growth of this tumor by 40%–70% compared to controls under chronic treatment with the somatostatin analogue octreotide during 6 wk had been demonstrated previously (*17,18*). Eight male Lewis rats were inoculated with a suspension of pancreatic tumor cells as described before (*17*). Two weeks after tumor transplantation 95% of the rats showed a detectable tumor mass. When the tumors had reached a solid palpable mass, the animals were used for the experiments. Nine male Lewis rats without tumor were used as controls. Iodine-123-Tyr-3-octreotide 18.5–37 MBq (1–3 μg), in 0.5–0.8 ml 154 m*M* NaCl and 0.05 *M* acetic acid were injected intravenously in tumor-bearing and control rats. The thyroids of the animals were not blocked. The radiopharmacon was injected in the dorsal vein of the penis. Two out of eight tumor-bearing rats received 1 mg octreotide subcutaneously 30 min before injection of ^{123}I-Tyr-3-octreotide in order to saturate somatostatin receptors on the tumors.

Data Acquisition and Analysis

Images were acquired with a large field of view gamma camera (Counterbalance 37 ZLC, Siemens Gammasonics) equipped with a 190-keV parallel-hole collimator. The animals were in a supine position on the collimator in such a way that overprojection of the tumor and the intestines was avoided. The analyzer was set to 159 keV with a 20% window. Data were stored in a dedicated computer (Gamma-11, Nuclear Diagnostics). In all animals (9 controls, 6 tumor-bearing animals without and 2 with octreotide pretreatment), acquisition took place for 40 intervals of 3 sec and 18 intervals of 60 sec (matrix 64 × 64) during the first 20 min of the study. After 30 min, static images were made containing 500K counts for a good quality image. Of four control animals and two tumor-bearing animals, additional static images (500K counts) were made 3 and 5 hr after injection; 24 hr after injection of the radiopharmacon another static image was made during 15 min. Static images were acquired in a 128×128 matrix and on X-ray film. In order to investigate the organ distribution of radioactivity, animals were killed 30 min (5 control and 2 tumor-bearing animals) and 24 hr (4 control and 2 tumor-bearing animals) after injection of the radiopharmacon and the radioactivity in the various tissues was measured with a GeLi-detector equipped with a multichannel analyzer (Series 40, Canberra). Tissues were not isolated from octreotide-pretreated animals.

One urine sample, collected from a tumor-bearing animal 30 min after injection, was used to investigate the radiochemical composition by HPLC (after 1:10 dilution in 40% methanol in 154 m*M* NaCl). Urine samples obtained 24 hr after injection from 2 tumor-bearing animals were analyzed on a SEP-PAK C18 cartridge.

RESULTS

Radiolabeling

In Figure 2, a typical elution pattern is presented of the purification of ^{123}I-Tyr-3-octreotide over a SEP-PAK C18 reversed-phase extraction cartridge. The radioactivity eluted with the ammonium acetate and water fractions appeared to be free radioiodide. The acetic acid fraction contained some peptide-bound radioiodine. The ethanol fraction contained 40%–60% of the applied radioactivity when ^{125}I was used for the labeling and 70%–80% when ^{123}I was used. Usually the specific activity of the SEP-PAK C18-purified ^{123}I-Tyr-3-octreotide reached a value of 30–37 MBq/μg peptide. Occasionally, labeling yields of 5% were observed after labeling with ^{123}I (see Discussion). With high labeling yields, the SEP-PAK C18 separations resulted in >99% peptide-bound radioiodine. HPLC analysis of the material in the ethanol fraction is shown in Figure 3A–B. After labeling with ^{125}I, two major peaks (at 19 and 21

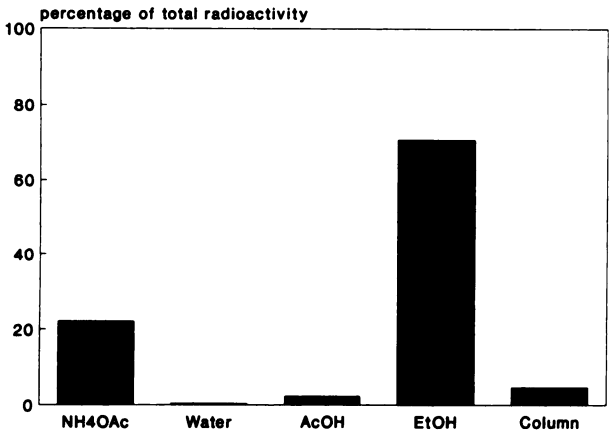

FIGURE 2
SEP-PAK C18 elution pattern after radioiodination of Tyr-3-octreotide.

min) were seen (Fig. 3A), of which the first one represents the mono-iodinated peptide (*12*) and the second probably the di-iodinated compound (see Discussion). With ^{123}I, usually over 99% of the labeled product consisted of mono-iodinated Tyr-3-octreotide (Fig. 3B), whereas in cases of low labeling yields, mentioned above, radioactivity was clearly present as di-iodinated peptide as well (up to 70% of total peptide-bound activity). For all further experiments, at least 99% radiochemically pure mono-iodinated Tyr-3-octreotide was used.

It was not possible to detect the low peptide mass of radioiodinated Tyr-3-octreotide along with the radioactivity in the elution profiles presented in Figure 3 (using either ^{123}I or ^{125}I). Furthermore, "cold" mono-iodinated ^{127}I-Tyr-3-octreotide and di-iodinated ^{127}I-Tyr-3-octreotide were not available. However, a clear separation between mono-radioiodinated (retention time 19 min) and unlabeled Tyr-3-octreotide (retention time 15 min) by HPLC was demonstrated.

In an attempt to increase the labeling efficiency with ^{125}I, a range of higher chloramine-T concentrations was tested. These radiolabeling procedures led not only to a substantial lowering of the labeling efficiency but also to a lower specific biologic somatostatin response measured as inhibition of the growth hormone secretion in rat pituitary cell cultures (data not shown). This is probably due to oxidative damage of Tyr-3-octreotide at high chloramine-T concentrations.

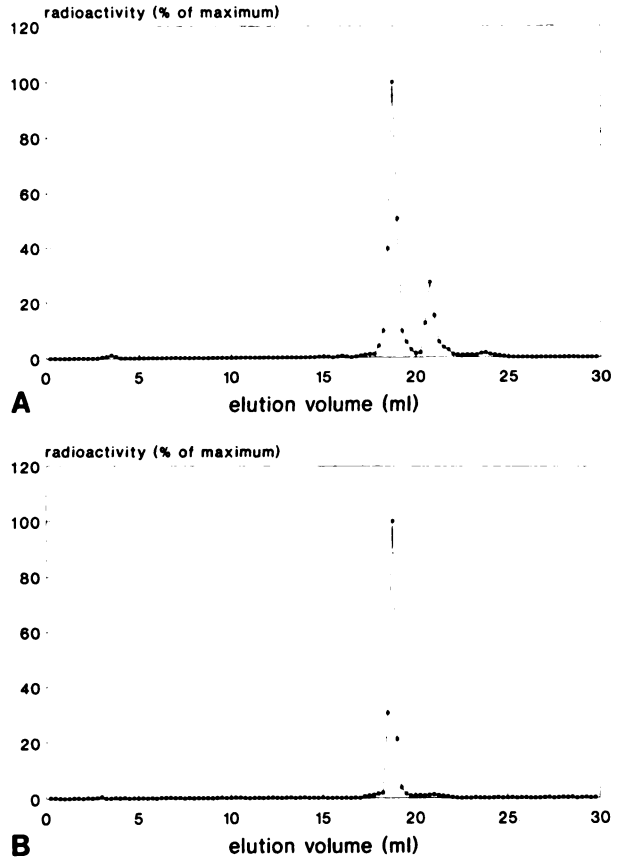

FIGURE 3
HPLC elution patterns after labeling Tyr-3-octreotide with ^{125}I (A) and Tyr-3-octreotide with ^{125}I (B).

Receptor Binding and Specific Biologic Activity

In Figure 4, the binding characteristics of radiolabeled Tyr-3-octreotide to human meningioma membranes are illustrated. Scatchard analysis of the data (inset Fig. 4) showed a dissociation constant K_d of 1.50 n*M* (r = 0.96) and a receptor concentration (B_{max}) of 98 fmol/mg of membrane protein, values similar to those reported for ^{125}I-Tyr-11-somatostatin (*13*).

Radiolabeled Tyr-3-octreotide showed the same biologic activity as octreotide and somatostatin. In Table 1, the secretion of rat growth hormone (rGH) by cultured rat pituitary cells is shown as a function of added Tyr-3-octreotide, HPLC-purified mono-iodinated ^{125}I-Tyr-3-octreotide, and somatostatin. The inhibition of rGH secretion by all three peptides was very similar. The presence of the radionuclide ^{125}I in the peptide did not disturb the results of the rGH radioimmunoassay.

Animal Studies

Dynamic scintigraphy of control rats after i.v. administration of ^{123}I-Tyr-3-octreotide showed a fast disappearance of the radioactivity from the blood circulation. Measurements with the gamma camera above the heart region showed that the time required to reach 50% of the highest radioactivity in the blood circulation was less than 2 min. Thirty minutes after injection static images showed clear appearance of radioactivity in the liver and intestines. The left kidney was seen as well as excreted activity in the bladder. The right kidney was not visible because of overprojection of the intestines. The accumulation of the radiolabeled Tyr-3-octreotide in the liver was immediately followed by hepatobiliary

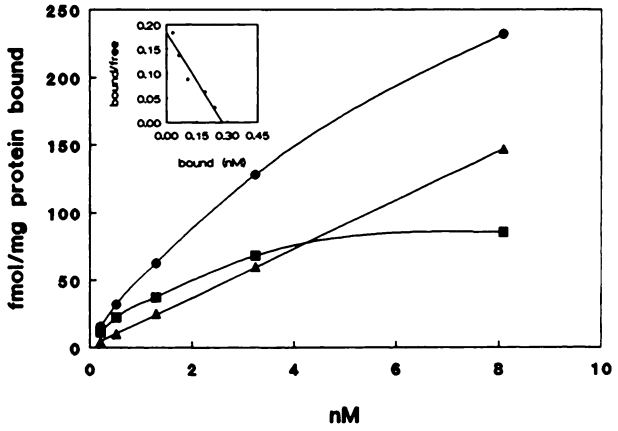

FIGURE 4
Saturation curve of radiolabeled Tyr-3-octreotide binding to human meningioma membranes: (●) total binding in absence of 10 μM somatostatin, (■) nonspecific binding in presence of 10 μM somatostatin and (▲) specific binding. Points are average of triplicates. Inset: Scatchard plot.

TABLE 1
Biologic Activity of (HPLC-purified) ^{125}I-Tyr-3-octreotide*

Peptide	Concentration (n*M*)	Rat growth hormone (ng/ml ± s.d.) (%)
^{125}I-Tyr-3-octreotide	0	296 ± 11 (100)
	0.05	299 ± 6 (101)
	0.1	220 ± 7 (74)
	0.5	188 ± 21 (64)
	1.0	184 ± 22 (62)
Tyr-3-octreotide	0	303 ± 11 (100)
	0.05	282 ± 11 (93)
	0.1	285 ± 13 (94)
	0.5	204 ± 13 (67)
	1.0	172 ± 19 (57)
Somatostatin	0	344 ± 18 (100)
	0.05	290 ± 27 (84)
	0.1	267 ± 24 (77)
	0.5	185 ± 18 (54)
	1.0	158 ± 8 (46)

* Secretion of rat growth hormone from cultured rat pituitary cells; (n = 4) by radiolabeled Tyr-3-octreotide, Tyr-3-octreotide, and somatostatin.

excretion. Thirty minutes after injection no further radioactivity accumulation was seen elsewhere. Two hours after injection the thyroid was visible. The main radioactivity at that time was situated in the intestines, while activity in the bladder was also seen. Five and 24 hr after injection the radioactivity in the thyroid was further increased. Although after 24 hr, the highest activity was found in the thyroid, a similar amount was spread diffusely over the intestines, but little radioactivity was seen in other tissues at that time.

The tissue radioactivity distributions in control rats, 30 min and 24 hr after i.v. injection of ^{123}I-Tyr-3-octreotide, were analyzed by radioactivity measurements of the various organs with a GeLi-detector. Thirty minutes after injection most of the administered radionuclide was located in the intestines, the liver, and the kidneys, while the highest radioactivity concentrations (% dose/g tissue) were found in the intestines, the adrenals, the kidneys and the liver (Table 2). However, even much higher concentrations of radioactivity were found in the collected urine specimens 30 min after injection. Twenty-four hours after injection the highest activities were measured in the thyroid and the intestines, with the thyroid having the highest concentration of radioactivity (Table 3). Urine samples were not collected 24 hr after injection.

In tumor-bearing rats, accumulation of the radioiodinated Tyr-3-octreotide at tumor sites could be demonstrated with the gamma camera. The scintigrams demonstrate a clear visualization of tumors at 30 min, 3, and 5 hr after injection. However, 24 hr after injection the previously accumulated radioactivity at the tumor sites had disappeared, which was confirmed by counting the isolated tumors 30 min and 24 hr after injection (data not shown).

TABLE 2
Tissue Distribution in Five Rats 30 min after Intravenous Administration of ^{123}I-Tyr-3-octreotide

Tissue	% dose (mean ± s.d.)	% dose/g (mean ± s.d.)
Intestines	50 ± 10	2.7 ± 0.5
Liver	12 ± 2	1.3 ± 0.2
Kidneys	3.5 ± 0.5	1.5 ± 0.3
Lungs	0.44 ± 0.12	0.37 ± 0.07
Spleen	0.10 ± 0.07	0.20 ± 0.12
Heart	0.10 ± 0.02	0.11 ± 0.01
Adrenals	0.06 ± 0.01	1.6 ± 0.3
Parotis	0.06 ± 0.03	0.11 ± 0.04
Thymus	0.048 ± 0.008	0.11 ± 0.02
Thyroid	0.004 ± 0.006	0.15 ± 0.06
Rest	26 ± 5	0.13 ± 0.02
Blood		0.24 ± 0.05
Urine		16 ± 13

Figure 5 shows a posterior view of a rat with somatostatin receptor-positive tumors to the left (320 mm^2) and to the right (144 mm^2) 30 min after injection, whereas at the same time point in a rat pretreated with 1 mg octreotide subcutaneously 30 min before injection of ^{123}I-Tyr-3-octreotide an even larger tumor at the left (640 mm^2) was only visible as vascular tissue radioactivity (Fig. 6).

A significant increase in radioactivity was demonstrated above nine tumors in six animals immediately after i.v. injection. Because of different sizes of tumors (and normal tissues) in various animals, normalization of data was necessary. The measured radioactivity during the first minute after injection was taken as a reference. Figure 7 shows the radioactivity as a function of time measured above nine tumors in six animals, expressed as percentage of the 1-min value. In Figure 7 is also shown that the above tumors in two rats (of which one is depicted in Fig. 6), which were pretreated subcutaneously with 1 mg octreotide 30 min before

TABLE 3
Tissue Distribution in Four Rats 24 hr after Intravenous Administration of ^{123}I-Tyr-3-octreotide

Tissue	% dose (mean ± s.d.)	% dose/g (mean ± s.d.)
Intestines	9 ± 10	0.6 ± 0.7
Liver	0.31 ± 0.03	0.027 ± 0.005
Kidneys	0.26 ± 0.04	0.10 ± 0.01
Lungs	0.040 ± 0.011	0.033 ± 0.006
Spleen	0.011 ± 0.010	0.028 ± 0.021
Heart	0.007 ± 0.002	0.009 ± 0.002
Adrenals	0.0028 ± 0.0007	0.07 ± 0.02
Parotis	0.0045 ± 0.0020	0.009 ± 0.004
Thymus	0.006 ± 0.003	0.016 ± 0.007
Thyroid	7 ± 2	180 ± 50
Rest	3.0 ± 0.6	0.016 ± 0.004
Blood		0.020 ± 0.006

FIGURE 5
Scintigraphy of a rat with one somatostatin receptor-positive tumor at the left (surface: 320 mm^2) and one at the right (144 mm^2), 20 min after i.v. injection of radiolabeled Tyr-3-octreotide. Apart from tumors (T) and bladder (B) activity is seen in heart, liver, intestines (including right kidney), and the left kidney.

FIGURE 6
Scintigraphy of a rat pretreated with 1 mg octreotide with one somatostatin receptor-positive tumor at the left (surface: 640 mm^2) 20 min after i.v. injection of radiolabeled Tyr-3-octreotide. (See also Fig. 5 legend.)

injection of the radiopharmacon, a decrease of radioactivity with time was measured similar to control tissues in eight animals reflecting the decreasing vascular tissue radioactivity.

Compared to the uptake in the liver the initial increase of radioactivity above the tumors was clearly higher in six tumors, equal in two tumors, and less in one tumor.

The tissue radioactivity distribution in tumor-bearing rats was similar to that in control rats both 30 min and 24 hr after ^{123}I-Tyr-3-octreotide injection (data not shown).

The biodistribution of the radiopharmacon in octreotide-pretreated animals showed a similar pattern as in the animals not pretreated with octreotide (including the controls), according to gamma camera measurements.

A 30-min urine sample was obtained from one tumor-bearing animal. HPLC-analysis of that sample showed that ^{123}I-Tyr-3-octreotide was excreted in unchanged form. Extraction of urine samples obtained 24 hr after injection from two tumor-bearing animals with a SEP-PAK C18 cartridge showed that more than 95% of the radioactivity was free radioiodide.

DISCUSSION

Tyr-3-octreotide is a stable analogue of somatostatin that can be easily radioiodinated (*12*). In this study, the postulate is tested that radioiodinated Tyr-3-octreotide, which has been used successfully in detecting somatostatin receptors in isolated tissues (*12,19,20*), is also suitable for in vivo imaging of tumors containing somatostatin receptors with ^{123}I as a radiolabel. For this, we investigated the radiolabeling of Tyr-3-octreotide (^{123}I compared with ^{125}I), the purification of the radiolabeled product, its specific biologic characteristics, in vivo metabolism, and application for imaging somatostatin receptor-positive tumors in the rat.

With ^{125}I, always consistent labeling yields of 40%–60% are obtained at a peptide:iodide ratio of 3:2. Because of the very high specific activity of ^{123}I, a large excess of Tyr-3-octreotide over total iodide can be used while keeping the absolute amount of peptide low (peptide:iodide = 100:3). In general, very high labeling yields (70%–80%) with high specific activities are obtained using ^{123}I. Occasionally, however, very low radi-

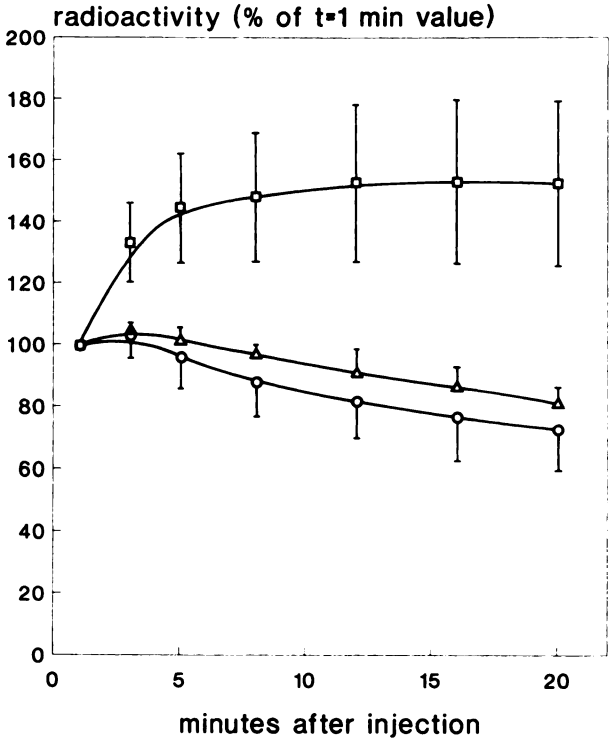

FIGURE 7
Radioactivity as a function of time, expressed as percentage (± s.d.) of the 1-min value, measured above nine tumors in six rats (□), two tumors in two rats, which were pretreated with 1 mg octreotide (△), and control tissues in eight animals (○).

olabeling yields (below 5%) are observed with ^{123}I. These difficulties are never seen when completely carrier-free ^{125}I (Amersham, England) is used. In the case of ^{123}I, other iodine isotopes (e.g., ^{125}I and stable ^{127}I) are contaminating the ^{123}I-preparation (maximal seven other iodine atoms versus one ^{123}I atom at the time of labeling) as a consequence of the radionuclide production method. The occasionally observed labeling yields below 5% are caused by production problems by which the product specifications (>3.7 TBq ^{123}I/mg iodine) are not met (see also below). The best and constant results are finally obtained with ^{123}I obtained from Medgenix (Fleurus, Belgium).

The high peptide-to-iodide ratio (100:3) favors not only a high labeling yield but also the formation of mono-iodinated over di-iodinated Tyr-3-octreotide. Radioactivity in the first HPLC-eluted peptide peak representing the mono-iodinated ^{123}I-compound usually was more than 99% of the total peptide radioactivity. This is in contrast to the ^{125}I-labeling (with a much lower peptide:iodide ratio of 3:2), where the second HPLC-eluted di-iodinated product always represents at least 30% of the total peptide-bound radioactivity, and HPLC is necessary to isolate the mono-iodinated peptide. A similar separation of radioiodinated Tyr-3-octreotide in two components has been reported previously (*12*) using ^{125}I as radiolabel and a different HPLC system. The occasionally low labeling yields with ^{123}I are always associated with formation of relatively much di-iodinated Tyr-3-octreotide (up to 70% of all peptide-bound radioactivity) because of the unexpectedly high amount of stable ^{127}I in the radionuclide preparation, which was afterwards confirmed by the manufacturer. Clearly a large excess of Tyr-3-octreotide compared to total iodide guarantees a high labeling yield and the formation of mainly mono-iodinated ^{123}I-Tyr-3-octreotide, of which high binding to somatostatin receptors was reported (*12*). Thus, it appears that the SEP-PAK C18 separation technique is adequate to prepare high activities (e.g., more than 2 GBq) of mono-iodinated ^{123}I-Tyr-3-octreotide.

The specific radioactivity of the ^{123}I-labeled peptide isolated on SEP-PAK C18 is proven to be high enough to demonstrate specific binding to human meningioma membranes. This suggests that additional HPLC purification is not necessary for the large amounts of radioactivity required for routine i.v. administration.

To demonstrate the specific biologic activity of the radiolabeled compound, the latter has been isolated by HPLC; it inhibits growth hormone release to a similar extent as Tyr-3-octreotide and somatostatin. This indicates that the radiolabeling procedure is not deleterious to the biologic activity of the peptide. In this case, mono-iodinated ^{125}I-Tyr-3-octreotide has been isolated, of which the specific radioactivity can be exactly calculated. This is not possible with ^{123}I because of the contamination with variable and unknown amounts of other iodine isotopes (see above).

In vivo disposal of circulating radioiodinated Tyr-3-octreotide in both control and tumor-bearing rats occurs predominantly by rapid hepatic clearance and biliary excretion as demonstrated with the scintigraphic studies and analyses of radioactivity in isolated tissues. This finding is in accordance with studies with octreotide itself (*21*) and another somatostatin analogue in the rat model (*22*).

A second route of clearance via the kidneys is demonstrated at 30 min on the scintigrams (left kidney and bladder) and organ distributions (Table 2). Note the very high radioactivity concentration in the urine samples collected at that time. The identification of urinary radioactivity in the form of unchanged radioiodinated Tyr-3-octreotide in a 30-min sample demonstrates that the compound is cleared intact by the kidneys. Of the low radioactivity in the 24-hr samples at least 95% is in the form of free radioiodide. The appearance of radioiodide in the urine is explained by complete hydrolysis of the labeled peptide followed by deiodination of iodotyrosine. A relatively high amount (7%–11%) of injected radioiodine is trapped in the thyroid after 24 hr, since the thyroids of the animals were not blocked.

The relatively high adrenal radioactivity concentra-

tion found 30 min after injection in control and tumor-bearing animals is in accordance with reported autoradiographic experiments (*20*), demonstrating the existence of somatostatin receptors in the rat adrenal.

The observed rapid decrease in circulating radioactivity of the radiopharmaceutical may benefit the sensitivity of the scintigraphic detection technique, especially as the receptor-bound radioactivity is stable once binding has taken place. This will result in a higher tumor/background ratio. For in vivo experiments, radioiodinated Tyr-3-octreotide is injected intravenously in rats with transplantable rat pancreatic tumors (CA 20948), which are known to contain somatostatin receptors in vitro (*16–18*). The increasing radioactivity measured above the tumor sites immediately after injection contrasts with the decreasing blood-pool radioactivity, which excludes imaging of the tumors solely on the basis of blood-pool radioactivity. This increase is usually more pronounced than that above the liver, which is an indication of a very rapid binding process. Obviously, the total maximum radioactivity above the liver is higher due to its greater size.

The specificity of the binding of ^{123}I-Tyr-3-octreotide to the tumors is most firmly established by the observation that pretreatment of the tumor-bearing rats with a high dose (1 mg) of octreotide (without changing the biodistribution of the radiopharmacon unchanged as observed with the gamma camera) results in a complete inhibition of the binding of label to the tumors. Consequently, immediately after injection decreasing radioactivity is measured over the blocked tumors, reflecting the radioactivity in the vascular pool, in contrast to the increasing radioactivity measured over the unblocked tumors (Fig. 7).

CONCLUSION

The radioiodination of Tyr-3-octreotide and the described purification procedure do not alter the specific somatostatin characteristics of the original compound, which means that this radiopharmaceutical is suitable for scintigraphic imaging of somatostatin receptors in vivo.

The fast disappearance from plasma of radioiodinated Tyr-3-octreotide after i.v. administration rapidly reduces the background level in the circulation, enhancing the possibility of scintigraphic imaging of somatostatin receptor-bearing tumors.

Because of the successful scintigraphic demonstration of somatostatin receptor-bearing tumors in the rat model using radioiodinated Tyr-3-octreotide, application of this new radiopharmaceutical in humans is promising since it is known that various human tumors possess large numbers of high-affinity somatostatin receptors, as demonstrated with ^{125}I-Tyr-3-octreotide in vitro (*11,13*).

ACKNOWLEDGMENTS

The authors thank Fred den Holder, Marion de Jong, Ina Loeve, Marcel van der Pluijm, Buddy Setyono-Han, and Frank van der Spek for their technical assistance.

REFERENCES

1. Hodgson HJF, Maton PN. Carcinoid and neuroendocrine tumours of the liver. *Baillière's Clinical Gastroenterology* 1987; 1:35–61.
2. Reichlin S. Somatostatin. *N Engl J Med* 1983; 309:1495–1501 and 1556–1563.
3. Schally AV. Oncological applications of somatostatin analogues. *Cancer Res* 1988; 48:6977–6985.
4. Pless J, Bauer W, Briner U, et al. Chemistry and pharmacology of SMS 201-995, a long-acting analogue of somatostatin. *Scand J Gastroenterol* 1986; 21(suppl 119):54–64.
5. Del Pozo E, Neufeld M, Schlutter K, et al. Endocrine profile of a long-acting somatostatin derivative SMS 201-995. Study in normal volunteers following subcutaneous administration. *Acta Endocrinol* (Copenhagen) 1986; 111:433.
6. Kvols LK, Moertel CG, O'Connell MJ, Schut AJ, Rubin J, Hahn RG. Treatment of the malignant carcinoid syndrome: evaluation of a long-acting somatostatin analogue. *N Engl J Med* 1986; 315:663.
7. Reubi JC. A somatostatin analogue inhibits chondrosarcoma and insulinoma tumor growth. *Acta Endocrinol* 1985; 109:108–114.
8. Lamberts SWJ, Reubi JC, Uitterlinden P, Zuiderwijk J, van der Werf P, van Hal P. Studies on the mechanism of action of the inhibitory effect of the somatostatin analog SMS 201-995 on the growth of the prolactin/adrenocorticotropin-secreting pituitary tumour 7315a. *Endocrinology* 1986; 18:2188–2194.
9. Lamberts SWJ, Koper JW, Reubi JC. The potential role of somatostatin analogs in the treatment of cancer. *Eur J Clin Invest* 1987; 17:281–287.
10. Lamberts SWJ, Uitterlinden P, Verschoor L, van Dongen KJ, del Pozo E. Long-term treatment of acromegaly with the somatostatin analogue SMS 201-995. *N Engl J Med* 1985; 313:1576–1580.
11. Reubi JC, Hacki WH, Lamberts SWL. Hormone-producing gastrointestinal tumours contain high density of somatostatin receptors. *J Clin Endocrinol Metab* 1987; 65:1127–1134.
12. Reubi JC. New specific radioligand for one subpopulation of brain somatostatin receptors. *Life Sci* 1985; 36:1829–1836.
13. Reubi JC, Maurer R, Klijn JG, et al. High incidence of somatostatin receptors in human meningiomas: biochemical characterization. *J Clin Endocrinol Metab* 1986; 63:433–438.
14. Scatchard G. The attractions of proteins for small molecules and ions. *Ann NY Acad Sci* 1949; 51:660–672.
15. Oosterom R, Verleun T, Zuiderwijk J, Lamberts S. Growth hormone secretion by cultured rat anterior pituitary cells. Effects of culture conditions and dexamethasone. *Endocrinology* 1983; 113:735–741.
16. Reubi JC, Horisberger U, Essed CE, Jeekel J, Klijn JGM, Lamberts SWJ. Absence of somatostatin receptors in human exocrine pancreatic adenocarcinomas. *Gastroenterology* 1988; 95:760–763.
17. Klijn JGM, Setyono-Han B, Bakker GH, Henkelman MS, Portengen H, Foekens JA. Effects of somatostatin analog (Sandostatin) treatment in experimental and human cancer. In: Klijn JGM, Paridaens R, Foekens JA, eds. *Hormonal manipulation of cancer: peptides, growth factors and new (anti) steroidal agents, EORTC Monograph Series, Volume 18*. New York: Raven Press; 1987:459–468.

18. Klijn JGM, Setyono-Han B, Bakker GH, Portengen H, Foekens JA. Prophylactic neuropeptide-analog treatment of a transplantable pancreatic tumor in rats. In: Bresciani F, King RJB, Lippman ME, Raynaud JP, eds. *Progress in cancer research and therapy, Volume 35, Hormones and Cancer 3.* New York, Raven Press; 1988:550–553.
19. Reubi JC, Maurer R. Autoradiographic mapping of somatostatin receptors in the rat central nervous system and pituitary. *Neuroscience* 1985; 15:1183–1193.
20. Maurer R, Reubi JC. Somatostatin receptors in the adrenal. *Molec Cell Endocrinol* 1986; 45:81–90.
21. Lemaire M, Andres H, Marbach P. Disposition of Sandostatin (SMS 201-995) in the rat. *Pharmaceut Weekbl* (Scientific Edition) 1988; 10:52.
22. Baker JR, Kemmenoe BH, McMartin C, Peters GE. Pharmacokinetics, distribution and elimination of a synthetic analogue of somatostatin in the rat. *Regul Pept* 1984; 9:213–226.
23. Veber DF, Holly FW, Nutt RF, et al. Highly active cyclic and bicyclic somatostatin analogues of reduced size. *Nature* 1979; 280:512–514.
24. Veber DF, Freidinger RM, Schwenk-Perlow D, et al. A potent cyclic hexapeptide analogue of somatostatin. *Nature* 1981; 292:55–58.

15 30

Selected manuscripts from the issues of The Journal of Nuclear Medicine published 15 and 30 years ago.
Edited by F.F. Mand

SEPTEMBER 1960

The Clinical Importance of Erythrocyte and Plasma-Volume Determinations Before and After Open-Heart Surgery

Edward A. Carr, Jr., MD, Herbert E. Sloan, Jr., MD, and Enrique Tovar, MD

A comparison of pre- and postoperative blood volumes in patients subjected to cardiotomy may have intrinsic interest to the physiologist and provide useful information for the postoperative management of the patients.

In the present study, the blood volumes of 17 patients before and after cardiotomy with extracorporeal circulation were compared. We determined both erythrocyte and plasma volumes directly in the majority of instances, making the postoperative determinations on the day following surgery. We have attempted to answer the following three questions. What are the size and direction of the changes in red cell and whole-blood volume observed? Do the changes observed correlate in any way with the postoperative course of the patients? How do the measurements obtained by the isotope method compare with those obtained by simple collection and direct measurement of lost blood?

For the accurate determination of plasma volume and total erythrocyte volume, standard isotope dilution methods were employed. Plasma volume was determined by the use of ^{131}I-labeled human serum albumin and total erythrocyte volume by the use of ^{51}Cr labeling of the patient's own erythrocytes.

The postoperative course of each patient was graded by review of the entire postoperative record after discharge or death of the patient.

The answer to the first two questions posed were conveniently given together. The mean total red cell volume was decreased postoperatively. The mean change, as determined by the radioisotope method, was −799 ml and, as calculated from "clinical estimation," −805 ml. The s.d. of the differences was ±733 ml. The t-test showed that this difference was not significant.

The mean whole-blood volume also decreased postoperatively. The mean change, as determined by the radioisotope method, was −733 ml, and as found by "clinical estimation," −94 ml. The s.d. of the differences was significant, ±898 ml.

There was a significant correlation between postoperative course and changes in whole-blood volume, as determined by the radioisotope method. There was no significant correlation between postoperative course and the "clinical estimation" of changes in whole-blood volume. ■

SEPTEMBER 1975

Myocardial Uptake of Labeled Oleic and Linoleic Acids

William H. Beierwaltes, Rodney D. Ice, Michael J. Shaw, and U. Yun Ryo

Since Bing et al. demonstrated that the rate of fatty acid extraction by the myocardium depends on the concentration of the fatty acids in the blood, we have tried to increase the uptake of labeled fatty acids in the myocardium. We were interested in ^{131}I-OA because the fatty acids offer the opportunity to detect biochemical as well as metabolic defects in the myocardium in addition to coronary insufficiency.

Forty-five Sprauge-Dawley rats were given ^{14}C-OA, ^{131}U-OA, or ^{131}I-LOA intravenously. Three rats in each of these groups were killed at 5-, 10-, 20-, 30-, and 50-min intervals. Three aliquots of each tissue were removed for radioactivity measurements. Iodinated fatty acids were also given intravenously to 12 adult mongrel dogs and similar procedures were performed.

Peak concentration of radioactivity in the blood from ^{14}C-OA and ^{131}I-OA was observed at 10 min. The radioactive concentration of ^{14}C-OA in the myocardium was significantly higher than that of the blood or other background tissues but was always lower than that in liver except 60 min after the dose when radioactivity in the myocardium was slightly higher.

Our data exhibit significant differences in the distribution (and metabolism) between ^{14}C-OA and ^{131}I-OA. These differences suggest that the mechanism of tissue "uptake" of iodinated oleic acid may be different from unlabeled oleic acid.

The relative tissue distribtuion of ^{131}I-OA radioactivity in the dog at 30 min after the i.v. dose demonstrated radioactivity in the ventricular myocardium about three times higher than that in the liver and four times higher than in the blood. This concentration in the blood was sufficient to obtain distinct images of the heart, using an Anger camera after i.v. administration of 0.5-1 mCi of ^{131}I-OA. We believe, however, that the amount of blood in the ventricular chamber contains sufficient activity to prevent separate imaging of ventricular myocardial ischemia. ■